

23rd International Conference on Material Forming (ESAFORM 2020)

Influence of a Hydrostatic Pressure Shift on the Flow Stress in Sheet Metal

Sam Coppieeters^{a*}, Mathias Jackel^b, Christian Kraus^b, Toshihiko Kuwabara^c and Frederic Barlat^d

^a KU Leuven, Technology Campus Ghent, Ghent, Belgium

^b Fraunhofer Institute for Machine Tools and Forming Technology IWU, Dresden, Germany

^c Tokyo University of Agriculture and Technology, Tokyo, Japan

^d GIFT-POSTECH, Pohang, Republic of Korea

* Corresponding author. Tel. 0032(0)9 331 66 72 E-mail address: sam.coppieeters@kuleuven.be

Abstract

The stack compression test (SCT) and the strain-rate controlled hydraulic bulge test (HBT) enable to determine the large strain flow curve of sheet metal under an identical deformation mode and balanced biaxial tension. This equivalence should lead to identical flow behavior if plastic yielding is independent of the hydrostatic stress. However, a discrepancy is observed in the flow curves of DP600 steel sheet determined by the SCT and the HBT. In order to avoid uncertainty with respect to dissimilar test conditions, the average strain-rate in both material tests is carefully controlled. Additionally, evidence is provided that friction can be sufficiently minimized yielding a homogeneous SCT up to a true plastic strain of 0.3. Assuming reliable experimental data, the hypothesis that the hydrostatic pressure shift between the stress states in the SCT and the HBT causes the observed difference in flow behavior is scrutinized. Theoretical considerations regarding the effect of a superimposed hydrostatic pressure (i.e. putting a material under a pressure environment for a certain stress state) on the flow stress, as suggested by Spitzig et al. [1] and Spitzig and Richmond [2], are used to understand the effect of a pressure shift between two stress states on the flow stress. Finally, the theoretical considerations are experimentally validated using the discrepancy in flow behavior of DP600 measured by the SCT and the HBT.

© 2020 The Authors. Published by Elsevier Ltd.

This is an open access article under the CC BY-NC-ND license <https://creativecommons.org/licenses/by-nc-nd/4.0/>

Peer-review under responsibility of the scientific committee of the 23rd International Conference on Material Forming.

Keywords: sheet metal; stack compression test; hydraulic bulge test; pressure dependency

1. Introduction

It is common knowledge that the predictive accuracy of sheet metal forming simulations largely depends on the adopted material model. In addition, many of these processes generate severe plastic deformation. Obviously, standard tensile tests are of limited usefulness because necking limits uniform deformation. Several experimental techniques have been developed [3-7] to determine the large strain flow curve of sheet metal. In this paper, the focus is on the stack compression test (SCT) and the hydraulic bulge test (HBT). Both tests enable the determination of the large strain flow

curve of sheet metal under an identical deformation mode. In terms of stress state, assuming that:

- plastic yielding is independent from the hydrostatic pressure, and
- friction in the SCT can be sufficiently reduced,

then the SCT is equivalent to the HBT, i.e. in-plane balanced biaxial tension. The SCT, also referred to as through-thickness compression test [6], layer compression test [8] or multi-layer upsetting test [9], enables to suppress plastic instabilities hence enabling to probe large plastic strains. The stack can consist of small circular discs [8, 9] or square specimens [10]. A clear

2351-9789 © 2020 The Authors. Published by Elsevier Ltd.

This is an open access article under the CC BY-NC-ND license <https://creativecommons.org/licenses/by-nc-nd/4.0/>

Peer-review under responsibility of the scientific committee of the 23rd International Conference on Material Forming.

benefit in this regard is that the SCT requires only a small amount of test material, which can be locally removed to acquire the local flow behaviour. Friction between the stack and the compression platen is inevitable. A friction-hill analysis [10] shows that a small height to diameter (or width for bricks) ratio, referred to as aspect ratio in the remainder of this work, requires a correction for friction to obtain an accurate flow curve. The latter implies that the friction coefficient can be measured, and, more importantly, is constant during the SCT. Indeed, friction conditions might vary as lubrication deteriorates due to thinning of the film and extension of the surface. With the aid of the ring compression test, An and Vegter [10] showed that oiled PFTE film yields a constant frictional behaviour. Coppieters [9] adopted the modified two specimen method [11] to calibrate the coefficient of friction in the SCT of low carbon steel. Steglich et al. [6] and Merklein and Godel [8] did not correct for friction when subjecting magnesium alloys and steel sheets to the SCT, respectively. Despite this inconsistency with respect to the role of friction in the SCT, it is clear that the aspect ratio plays a crucial role in assessing the need for friction correction [10]. The lower the aspect ratio of the stack, the more pronounced the frictional effect and the need for friction correction. However, when targeting the large strain flow curve, a small aspect ratio is favoured for the stability of the stack deformation and mitigating preliminary stack defects such as disc localization. Moreover, frictional effects lead to a triaxial stress state which further complicates the determination of the flow curve. Obviously, friction is a disadvantage of the SCT. The crux of the problem is that one must be able to guarantee a strain range for which a constant frictional condition prevails. In addition, correction of the flow curve requires a method to quantify the frictional condition. When a shearable film (e.g. TPFE) is used, a correction can be made based on the shear strength of the film [10]. As opposed to the SCT, the HBT does not suffer from frictional effects but in turn lacks accuracy due to assumptions involved in the analytical treatment of the experimental data [7].

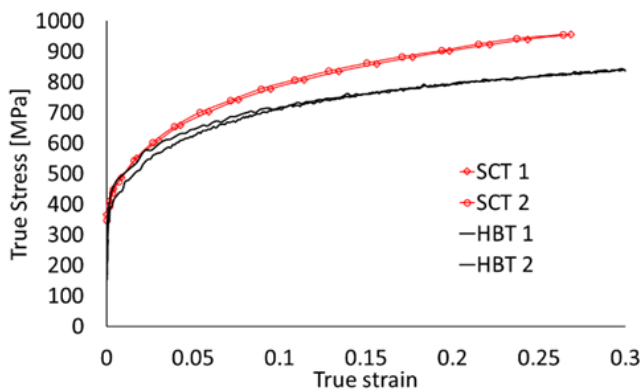


Fig. 1. Flow curves obtained through SCT and HBT.

In addition, it is well-known that the HBT is not accurate in determining the flow curve at moderately low plastic strains due to the uncertainty related to measuring the curvature of the dome apex. Given the identical deformation mode and stress condition, one would expect identical flow behaviour obtained through the SCT and HBT. Merklein and Godel [8] found a

good agreement between the SCT and HBT for DC04 and DX56 steel sheet. Mulder et al. [12] initially found a discrepancy between the SCT and the HBT for DC06. According to Mulder et al. [13], the latter discrepancy could be attributed to strain rate and temperature effects in the HBT. Steglich et al. [6] found an excellent agreement between the SCT and HBT for magnesium alloys. The aim of this paper is to further elaborate on the discrepancy between the SCT and the HBT found for DP600 steel sheet. The next section discusses the experimentally acquired flow behavior of DP600 determined using the SCT and the HBT. To probe large plastic strains with the SCT, a low aspect ratio is chosen along with a strategy to correct for friction. Based on the work by Spitzig et al. [1] and Spitzig and Richmond [2], Section 3 embarks on theoretical considerations regarding the role of the hydrostatic pressure shift on the flow stress. The latter findings are experimentally validated in Section 4 using the flow behaviour determined in Section 2. Conclusions are drawn in Section 5.

2. Experimental

2.1. SCT and HBT

The SCT is conducted on an electro-mechanical press with a load capacity of 100 kN. The stack consisted of 3 discs with a diameter of 10 mm. Lubrication (oil) is applied to minimize the effect of friction. The red curves shown in Fig. 1 show the experimentally acquired flow curves using the SCT calculated following:

$$\sigma_{avg}^c = \frac{F \cdot h}{\pi \cdot r_0^2 \cdot h_0} \quad (1)$$

where σ_{avg}^c is the average compressive true stress, F the measured force and h_0 , r_0 the initial stack height and radius, respectively. The logarithmic true compressive strain is simply:

$$\varepsilon = \ln\left(\frac{h_0}{h}\right) \quad (2)$$

It can be inferred that the SCT yields a good repeatability up to a true plastic strain of 0.3. Beyond that point, lubricant depletion led to metallic contact and galling is observed. Fig. 1 also shows the flow behaviour measured by the HBT. The HBT-flow stress is calculated as follows:

$$\sigma = \frac{\rho \cdot p}{2 \cdot t} \quad (3)$$

where σ and p are the true stress and fluid pressure, respectively. The logarithmic true strain is estimated as:

$$\varepsilon = -\varepsilon_1 - \varepsilon_2 \quad (4)$$

which is valid assuming equal strain or equal stress at the specimen pole. The radius of curvature ρ and the principal strains $\varepsilon_1, \varepsilon_2$ at the top of the bulged specimen are measured using a stereo DIC system. In this regard, ISO 16808 is followed and extended with a closed-loop strain rate control at the top of the dome. The average strain rates in the HBT and the SCT are both approximately $10^{-4} \frac{1}{s}$. It can be inferred from Fig.1 that the repeatability of the HBT beyond a true strain of 0.1 is excellent.

2.2. SCT: friction correction

Given the low aspect ratio of the stack, it is required to compensate for friction. The friction-hill analysis of a homogenous compression of a single disc [14] leads to:

$$\sigma = \frac{2 \cdot \sigma_{avg}^c}{\left(\frac{h}{\mu r}\right)^2 \cdot \left[e^{\frac{2\mu r}{h}} - \frac{2\mu r}{h} - 1 \right]} \quad (5)$$

with h , r the instantaneous height and radius of the stack, respectively. The height h of the stack is measured and r is derived assuming volume constancy. Eq.(5) is validated for the stack configuration (i.e. number of discs and diameter) adopted in this study using a FE model of the SCT. This means that Eq.(5) can be adopted to correct the SCT-flow curve shown in Fig. 1 provided that the friction coefficient μ is known. The modified two specimen method (MTSM) [11] could be adopted to identify μ . The fundamental hypothesis of the MTSM, however, is that the material behavior is independent of the stack configuration. Given that the hydrostatic stress component in the stack potentially depends on the stack configuration, the MTSM is not applied.

In this work, the coefficient of friction is inversely calibrated using an FE model of the SCT. To this end, the SCT is simulated using a displacement-driven FE model assuming a constant friction coefficient and adopting the HBT-flow curve which is considered here as the ground-truth strain hardening. The left panel of Fig. 2 shows the experimental cross section of the stack after compression, while the right panel shows the numerical simulation. A frictionless SCT would lead to a perfectly homogeneous experiment, instead some slight barreling can be observed in the left panel.

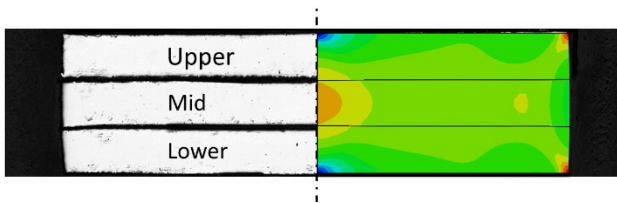


Fig. 2. Cross-section compressed stack DP600. Left: experimental. Right panel: FE simulation using HBT-flow curve and $\mu=0.05$.

Instead of assessing the homogeneity of the SCT by evaluating this barreling, one could also evaluate the thickness of each individual disc. Indeed, a frictionless experiment would lead to an identical thickness reduction of each disc in the stack. The red symbols in Fig. 3 show the experimentally measured (average of 3 experiments) disc thicknesses at the center of each disc. It can be inferred that the mid disc is consistently thinner than the discs that are in contact with the compression platens. This observation is used to inversely tune the friction coefficient using the FE model. Fig. 3 shows the numerically predicted thicknesses using three friction coefficients, namely $\mu=0.1$, 0.05 and 0.03 . It can be seen that a friction coefficient of $\mu= 0.05$ enables to accurately reproduce the thickness

reduction of the individual discs in the stack.

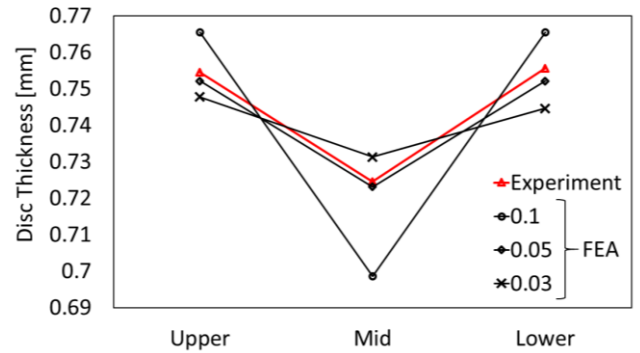


Fig.3. Thickness after compression measured at the centre of each individual disc

It must be noted that this is in line with the findings of Coppieters [9] using the MTSM. Fig. 4 shows the SCT-flow curve corrected for friction using Eq.(5) with a constant friction coefficient of $\mu= 0.05$. It can be seen that the corrected SCT-flow curve is bounded between the raw SCT-flow curve and the lower bound HBT-flow curve.

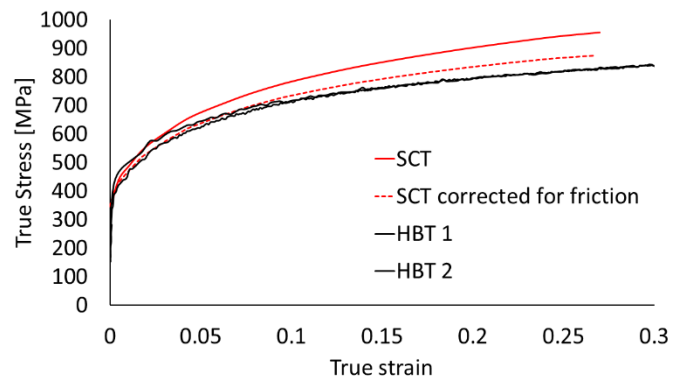


Fig.4. Flow curves obtained through SCT (with and without correction for friction) and HBT.

Theoretical

Given that the HBT-flow curve lacks accuracy in the strain range $0 \leq \epsilon \leq 0.15$, the focus here will be on the discrepancy of the flow behavior in the strain range $0.15 \leq \epsilon \leq 0.3$. Note that this analysis is inherently assuming a correct compensation for friction in the SCT. In this section, we draw on the work of Spitzig et al. [1, 2] regarding the effect of superimposed hydrostatic pressure on the tension and compression flow stress behavior of steels. They concluded that the hydrostatic pressure increases the yield strength and work hardening rate of steels. Richmond and Spitzig [15] used a yield condition enabling to describe their experimental observations, namely:

$$I_2 = c - aI_1 \quad (6)$$

where I_2 is the von Mises effective stress and I_1 the first stress tensor invariant. When the parameters a and c are constants, this yield condition is identical to that proposed by Drucker and Prager [16]. However, Spitzig and Richmond [1] revealed that a and c are strain dependent coefficients that can be determined from experiments. Additionally, they showed that the pressure coefficient α , which reads as:

$$\alpha = \frac{a}{c} \quad (7)$$

is nearly constant and within the range of $13 \leq \alpha \leq 23$ (TPa⁻¹) for a number (about 10) of low and high strength steels. Since the yield condition Eq.(6) enables the capture of the well-known strength differential effect (SDE), i.e. the difference between the flow stress under uniaxial tension and compression, this supports the idea that the SDE is driven by the interaction of pressure and the transient dilatancy of moving dislocations as demonstrated by Bulatov et al.[17]. Given that the yield condition Eq. (6) depends on the first stress tensor invariant, however, it is used here to understand the discrepancy in flow behavior between the SCT and the HBT. The stress states associated with the SCT and the HBT are σ^{SCT} and σ^{HBT} , respectively. Without a superimposed external pressure, the yield condition Eq.(6) can be applied to a material that is subjected to the stress states σ^{SCT} and σ^{HBT} , respectively:

$$I_2(\sigma^{SCT}) = c - aI_1(\sigma^{SCT}) \quad (8)$$

$$I_2(\sigma^{HBT}) = c - aI_1(\sigma^{HBT}) \quad (9)$$

Subtracting both equations, i.e. Eq.(8) - Eq.(9), yields:

$$I_2(\sigma^{SCT}) - I_2(\sigma^{HBT}) = -aI_1(\sigma^{SCT}) + aI_1(\sigma^{HBT}) \quad (10)$$

Note that this approach with the von Mises effective stress I_2 can be extended to any pressure independent effective stress $\bar{\sigma}$. The mean or hydrostatic stress σ_m is one third of the first stress tensor invariant yielding:

$$\bar{\sigma}(\sigma^{SCT}) - \bar{\sigma}(\sigma^{HBT}) = +3a [\sigma_m^{HBT} - \sigma_m^{SCT}] \quad (11)$$

Eq. (11) shows that the difference in the two effective stresses is proportional to the pressure shift between the two stress states σ^{SCT} and σ^{HBT} . Moreover, it shows that the difference in effective stress between the SCT and the HBT can be used to calibrate the parameter a of the yield condition, Eq. (6):

$$a = \frac{\bar{\sigma}(\sigma^{SCT}) - \bar{\sigma}(\sigma^{HBT})}{3 \cdot [\sigma_m^{HBT} - \sigma_m^{SCT}]} \quad (12)$$

By substituting the mean stresses, Eq.(12) reads as:

$$a = \frac{\bar{\sigma}(\sigma^{SCT}) - \bar{\sigma}(\sigma^{HBT})}{2\sigma^t + \sigma^c} \quad (13)$$

as $\sigma^t = \bar{\sigma}(\sigma^{HBT})$ for an isotropic material with σ^t the uniaxial tensile stress. Given that for steels, half of the strength-differential effect can be written as [15]:

$$\frac{\sigma^c - \sigma^t}{\sigma^c + \sigma^t} = a \ll 1 \quad (14)$$

the following relation between a and the difference in flow behaviour can be derived:

$$a = \frac{\bar{\sigma}(\sigma^{SCT}) - \bar{\sigma}(\sigma^{HBT})}{3 \cdot \bar{\sigma}(\sigma^{HBT})} \quad (15)$$

In other words, the flow curves measured with the aid of the SCT and the HBT can be exploited to identify the parameter a in Eq.(6). It must be noted that Eq. (15) must be evaluated at an instant when the same amount of plastic work per unit volume is consumed. Finally, the coefficient c can be calculated as:

$$c = \bar{\sigma}(\sigma^{HBT}) \cdot (1 + 2 \cdot a) \quad (16)$$

3. Results and discussion

The difference in flow behavior shown in Fig. 4 is used to calculate a and c in the strain range $0.15 \leq \varepsilon \leq 0.3$ following Eq.(15) and Eq.(16), respectively. According to Eq.(7), the values of a and c can be used to calculate the pressure coefficient α . For DP600, it can be inferred from Fig. 5 that α is nearly constant (average $\alpha = 20.5$ TPa⁻¹) and within the range of $13 \leq \alpha \leq 23$ (TPa⁻¹). The fact that α is not perfectly constant might be due the assumed constant frictional condition, an assumption which is potentially violated as lubrication depletes as the deformation increases. Although friction probably introduces some uncertainty here, it seems that the current findings are consistent with the work of Spitzig and Richmond [15] on high strength steels. As opposed to the findings obtained through exploiting the difference in flow behavior between the SCT and the HBT, in-plane tension-compression experiments enable to accurately determine the pressure coefficient α for sheet metal in the lower strain range, e.g. $0 \leq \varepsilon \leq 0.1$. Recently, Maeda et al. [18] correlated the SDE effect with the pressure dependent yield condition Eq.(6) for DP980 sheet. They calibrated the coefficients a and c for DP980 steel sheet using in-plane tension-compression

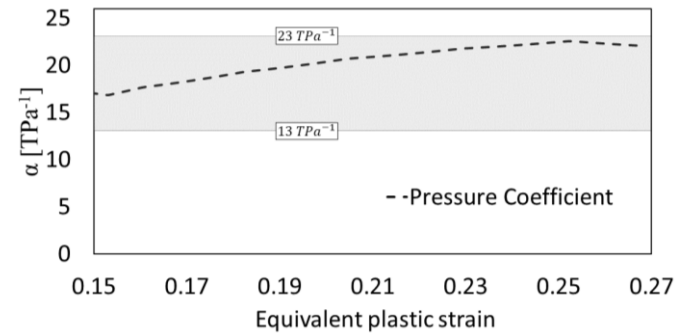


Fig.5. Pressure coefficient α (DP600) in the strain range $0.15 \leq \varepsilon \leq 0.3$

experiments and found a pressure coefficient α of 24 TPa⁻¹ associated with a true plastic strain of $\varepsilon = 0.08$. Shirakami et al. [19] measured the SDE effect of DP590 steel sheet and found that the compressive flow stress is higher than in tension by approximately 6% in the strain range $0 \leq \varepsilon \leq 0.05$. In this regard, Fig. 4 shows that in the strain range $0.15 \leq \varepsilon \leq 0.3$, the SCT-flow stress of DP600 steel is consistently higher than the HBT-flow stress by approximately 6%. As such, the work of Maeda et al. [18] and Shirakami et al. [19] for moderately small plastic strains seems to be in agreement with the findings here for larger plastic strain up to 0.3.

4. Conclusions

This study investigated the difference in flow behavior measured by the stack compression test and the strain rate controlled hydraulic bulge test of a dual phase steel sheet with a tensile strength of 635 MPa. It is shown, as suggested by Spitzig et al. [1] and Spitzig and Richmond [2] that the observed difference in flow behavior can be related to a hydrostatic pressure shift between the stress states that prevail in the stack compression test and the hydraulic bulge test. Moreover, the measured difference in flow behavior in those tests can be used to calibrate the pressure dependent yield condition. Despite the uncertainty regarding the friction in the SCT, the experimental measurements of the pressure coefficient α are in good agreement with the work of Richmond and Spitzig [15]. Future work will embark on numerical reproduction of the experimental findings using plasticity models enabling to describe the plastic behavior of incompressible, yet hydrostatic pressure sensitive metals, e.g. through the work of Aretz [20].

Acknowledgements

The presented results are part of the CORNET research project "Standardization of Flow Curve Determination for Joining by Forming" coordinated by European Research Association for Sheet Metal Working funded by the program for "Industrial Research" (IGF) of the Federal Ministry of Economics and Technology Germany and the Belgian government agency "Flanders Innovation & Entrepreneurship" (VLAIO).

References

- [1] Spitzig WA, Richmond O. The effect of pressure on the flow stress on metals. *Acta Metall* 1984;32:457-463.
- [2] Spitzig WA, Sober RJ, Richmond O. Pressure Dependence of yielding and associated volume expansion in tempered martensite. *Acta Metall* 1975; 23:885-893.
- [3] Coppieters S, Kuwabara T. Identification of post-Necking hardening phenomena in ductile sheet metal. *Exp Mech* 2014;54:1355-1371.
- [4] Traphöner H, Clausmeyer T, Tekkaya AE. Material Characterization for Plane and Curved Sheets Using the In-Plane Torsion Test – An Overview. *J Mater Process Technol* 2018;257:278-287.
- [5] Charles C, Unruh K, Peshekhodov I, Chottin J, Balan T. A New Analytical Method for Determination of the Flow Curve for High-strength Sheet Steels Using the Plane Strain Compression Test. *Int J Mater Form* 2019.
- [6] Steglich D, Tian X, Bohlen J, Kuwabara T. Mechanical testing of thin sheet magnesium alloys in biaxial tension and uniaxial compression. *Exp Mech* 2014; 54:1447-1258.
- [7] Mulder J, Vegter H, Aretz H, Keller S, van den Boogaard AH. Accurate determination of flow curves using the bulge test with optical measuring systems. *J Mater Proc Technol* 2015; 226:169–187.
- [8] Merklein M, Godel V. Characterization of the flow behavior of deep drawing steel grades in dependency of the stress state and its impact on FEA. *Int J Mater* 2009; 2-1:415-418.
- [9] Coppieters S. Experimental and numerical study of clinched connections, PhD thesis, KU Leuven, 2012.
- [10] An YG, Vegter H. Analytical and experimental study of frictional behavior in through-thickness compression test. *J Mater Process Technology* 2005;160:148-155.
- [11] Han H. The validity of mechanical models evaluated by two-specimen method under the unknown coefficient of friction and flow stress. *J Mater Process Technol* 2002;122:386-396.
- [12] Mulder J, Vegter H, Ha JJ, van den Boogaard AH. Determination of flow curves under equibiaxial stress conditions. *Key Eng Mater* 2012;504-506:53-58.
- [13] Mulder J, Vegter H, van den Boogaard AH. An engineering approach to strain rate and temperature compensation of the flow stress established by the hydraulic bulge test. *Key Eng Mater* 2015;651-653:138-143.
- [14] Dieter GE. *Mechanical Metallurgy*. McGraw-Hill Book Company, 1987, London.
- [15] Richmond O, Spitzig WA. Pressure dependence and dilatancy of plastic flow. IUTAM Conference, Theoretical and Applied Mechanics, Proc. 15th International Congress on Theoretical and Applied Mechanics 1980;377-386.
- [16] Drucker DC, Prager W. Soil mechanics and plastic analysis of limit design. *Q Appl Math* 1952;10: 157-165.
- [17] Bulatov VV, Richmond O, Glazov MV. An atomistic dislocation mechanism of pressure-dependent plastic flow in aluminium. *Acta Mater* 1999; 47: 3507-3514.
- [18] Maeda T, Noma N, Kuwabara T, Barlat F, Korkolis YP. Measurement of the strength differential effect of DP980 steel sheet and experimental validation using pure bending test. *J Mater Process Technol* 2018; 265: 247-253.
- [19] Shirakami S, Kuwabara T, Tsuru E. Axial compressive deformation behavior and material modelling of steel pipe with bending deformation history. *J JSTP* 2017; 58: 692-698 (in Japanese).
- [20] Aretz H. A consistent plasticity theory of incompressible and hydrostatic pressure sensitive metals. *Mech Res Commun* 2007; 34:344-351.